

On the importance of normal vibrations in modeling of stick slip in rock sliding

W. Woytek Tworzydło and Osama N. Hamzeh

Computational Mechanics Company, Inc., Austin, Texas

Abstract. In this paper, numerical studies of friction-induced dynamic instabilities, in particular, stick-slip sliding of rocks, are presented. Of special interest is the importance of normal compliance of the interface and associated normal vibrations in the occurrence of dynamic instabilities. To clearly illustrate this importance, the interface is represented by the Oden-Martins constitutive model which does not exhibit explicit velocity or slip dependence of friction. This friction model is utilized in the context of a rather simple rigid body model to perform numerical studies representative of granite blocks in relative sliding at very slow overall velocities. The model represents a common experimental setting that has been used to study stick slip of sliding rock blocks. To capture the stick-slip phenomenon the detailed dynamic response of this system is modeled numerically. These studies indicate the importance of the normal compliance of the interface on the stability of sliding. In particular, dynamic coupling of the degrees of freedom contributes to dynamic instability of the system and can cause stick-slip motion. Both stable and unstable sliding are predicted and examined.

1. Introduction

It is generally agreed among geophysicists that the main source of shallow earthquakes is the stick-slip phenomena that take place along portions of the interface between tectonic plates. When these plates, which are moving relative to each other at a very slow pace, stick at their interfaces, strain energy builds up in the surrounding medium. Considerable amounts of this energy are released by the sudden slip and then radiated by waves propagating in the surrounding crust. These stick-slip events are classified as unstable frictional phenomena. In addition, some jolts are caused by rock fracture.

Previous attempts of modeling stick-slip instabilities were based on friction laws that are explicitly slip-dependent or velocity-dependent (also referred to as slip- or velocity-weakening laws) [Andrews, 1976b; Biegel *et al.*, 1989; Byerlee, 1967; Cao and Aki, 1986; Carlson *et al.*, 1991; Dieterich, 1979a, b; Lockner *et al.*, 1986; Rice and Tse, 1986; Rice, 1982, 1993; Ruina, 1985; Stuart and Mavko, 1979]. These slip-dependent laws stemmed from the apparent displacement or slip weakening of friction which has been observed in many experimental works, a typical behavior of this type was studied by Byerlee [1967], Lockner *et al.* [1986], and Dieterich [1978, 1979a]. It was also used in the numerical simulations of Andrews [1976a, b], Stuart and Mavko

[1979], *Day* [1982a, b], and many others. A somewhat different, yet closely related, phenomenon is velocity dependence of friction, studied experimentally by *Stesky* [1978], *Dieterich* [1978, 1979a], *Ruina* [1983], *Tullis and Weeks* [1986], *Lockner et al.* [1986], *Biegel et al.* [1989], *Blanpied et al.* [1991], and others. As a phenomenological explanation of the velocity weakening of friction, *Dieterich* [1978] proposed dependence of friction on the average time of contact between the asperities on the opposing surfaces: lower velocities would allow for longer average contact time resulting in a higher value for the coefficient of friction. In experimental work on rubber blocks aimed at understanding the earthquake phenomenon, *Brune et al.* [1993] emphasized the importance of normal vibrations at the interface.

To incorporate the above experimental observations, various extensions of the classical Coulomb friction law have been proposed for rock friction. One of the most complete and complex of these models is the state-variable friction law developed by *Dieterich* [1979a] and consequently refined by *Ruina* [1983], *Rice and Ruina* [1983], and *Rice and Gu* [1983].

However, these friction laws were based on the assumption that the displacement or slip weakening observed in experiments on rock sliding is attributable entirely to the frictional properties of the interface. In other words, there is one-to-one correspondence between the velocity dependence of the shear traction on the fault surfaces with the apparent velocity-dependent force of the sliding test specimen. However, this has been shown not to be the case [see, e.g., *Aronov et al.*, 1983; *Oden and Martins*, 1985; *Tolstoi*, 1967; *Tolstoi et al.*, 1971; *Tworzydło and Becker*, 1991; *Tworzydło et al.*, 1992]. Indeed, it is a widely known fact that friction-velocity curves for the same surfaces obtained from different apparatuses are usually quite different. This observation can be attributed to the fact that macroscopic behavior of the sliding system is a consequence of both the tangential properties of the interface and the dynamic motion of the entire system, including vibrations normal to the interface. This has been demonstrated for technological systems (Man-made manufactured systems, such as machine parts, automotive components, etc.) in both experimental investigations [*Aronov et al.*, 1983; *Dweib and D'Souza*, 1990; *Tolstoi*, 1967; *Tolstoi et al.*, 1971] and in numerical simulations [*Oden and Martins*, 1985; *Tworzydło and Becker*, 1991; *Tworzydło et al.*, 1992].

The importance of the global dynamic behavior of the contact system as a whole and, in particular, normal vibrations of the slider, has not been widely recognized.

Tolstoi [1967] concluded in his early experimental work that once the normal vibrations of the moving system are suppressed by heavy damping, the difference between static and dynamic coefficients of friction vanishes. Realizing these facts, *Oden and Martins* [1985] introduced a constitutive model for frictional interfaces that uses a power law normal response and coefficient of friction with no explicit velocity dependence. This model, when combined with detailed analysis of the motion including high-frequency micro vibrations of the slider, is capable of producing many of the observed phenomena of friction, such as stick-slip motion.

It is of importance to note that we do not claim here that there is no velocity dependence of friction on the interface or that the Oden-Martins friction model can be used to explain all the intricate frictional phenomena on the fault surface. While it has been used successfully to predict behavior of some technological systems, the Oden-Martins model will certainly not suffice to represent gouge layers, long-term time-dependent effects, etc. However, this model is used in this paper to very clearly show that the normal oscillations on the interface can trigger or contribute to unstable sliding. It can be expected that in most practical systems, both velocity dependence of friction and normal compliance of the interface contribute to the instability of tangential sliding.

The objective of this research work is to clearly demonstrate the possibility of triggering unstable dynamic friction phenomena (namely, stick-slip) in the context of rock sliding by mechanisms other than explicit velocity dependence. It is the recognition of the role of the normal approach between the two contacting surfaces, combined with detailed dynamic analysis of the system, that can result in such instabilities. This has been shown in earlier work to be valid for technological systems; here we show it to be the case for rock blocks sliding at average velocities corresponding to typical tectonic creep.

In this paper, the Oden-Martins interface law is utilized in a spring-block model to study sliding behavior of granite blocks. Though this simple rigid block model does not represent actual fault systems, it resembles some simpler experimental settings, and it exhibits some interesting behavior observed in these experiments, such as stick-slip. A different approach, however, is undertaken here to model this behavior.

The dynamic behavior of the system during stick and slide phases is modeled by a fully nonlinear transient analysis. The Newmark- β method is used to solve the equations of motion. Owing to the disproportionate

timescales of events in the stick and slip phases, an adaptive time-stepping algorithm combined with a temporal error estimator is implemented. Similarly, the velocities involved in the stick and slip stages differ by orders of magnitude; therefore an adaptive sizing of the regularization region of the friction law is implemented. Illustrative numerical examples, with material properties relevant to granite blocks, are analyzed. The behavior on both the microscopic and the macroscopic levels is considered. The effects of the system stiffness and external damping on the stability of friction are briefly investigated. It is also shown that a potentially stable system can be triggered into unstable motions if subjected to a strong enough perturbation. In addition, some linearized stability analyses of the equations of motion at the steady state sliding equilibrium position of the block are presented.

2. A New Approach to Modeling of Friction-Induced Instabilities of Sliding Rock Formations

When two bodies in contact translate relative to each other along a contact boundary, the motion can be stable or unstable. In the stable case, the (apparent) coefficient of friction remains basically constant and the movement is of a steady state nature; that is, the two bodies slide at a constant relative velocity. On the other hand, in the unstable case, the relative motion of the two bodies alternates between stick (or very slow slip) periods and slip events, usually with different values of the coefficient of friction in stick and slip phases. The stick-slip motion and similar phenomena of friction have been traditionally modeled by explicit slip- or velocity-dependent friction. In these laws, the value of the coefficient of friction depends on the relative distance (or velocity) of slip in the tangential direction. Some more advanced laws may also involve the history of slip [*Rice*, 1982, 1993; *Ruina*, 1985].

In this work we explore a different approach, which is based on the recognition of the importance, to the stability of frictional sliding, of (1) both normal and tangential properties of the contact interface, and (2) dynamic coupling between oscillation modes of the system, which can promote instability.

In particular, it has been shown for technological systems that one of the mechanisms of friction-induced oscillations is caused by frictional coupling between normal and rotational oscillations of the system or its sub-components. Presence of friction causes coalescence of normal and rotational frequencies and unstable propa-

gation of vibrations. Such behavior has been illustrated in our previous analytical studies of dynamic friction phenomena [Oden and Martins, 1985; Oden et al., 1989; Tworzydło and Becker, 1991; Tworzydło et al., 1992, 1994] and has been confirmed in independent laboratory experiments [Aronov et al., 1983, 1984; D’Souza and Dweib, 1990; Dweib and D’Souza, 1990; Soom and Kim, 1983]. In the current work, we extend this research approach to transient studies of unstable frictional sliding of rock formations. As a result, it is suggested that to successfully model and predict unstable sliding on real fault systems, the modeling approaches need to be extended to include the following: (1) more general constitutive laws of the interface (slip surface), including both normal compliance and frictional characteristics with rate- and state-dependent behavior, (2) representative dynamic models of the system (possibly finite element models), including three-dimensional sliding bodies (rock formations) and the interface (fault surface), and (3) methods of modeling dynamically unstable motions.

3. A Constitutive Friction Model for the Interface

The constitutive equations of the interface applied in this work are based on the Oden-Martins model [Oden and Martins, 1985] and consist of two basic equations: a normal interface law and a friction law. For the normal response, instead of assuming a typical Signorini-type rigid contact condition, we model the normal compliance of the interface by

$$\begin{aligned} \sigma_N &= c_N a^{m_N} + b_N a^{l_N} \dot{a}, & a \geq 0, \\ \sigma_N &= 0, & a < 0, \end{aligned} \quad (1)$$

where σ_N is the normal stress (compression taken as positive), a is the normal approach (penetration) on the interface, and \dot{a} is its time derivative. Coefficients c_N , b_N , m_N , and l_N are positive and depend on the properties of the contacting surfaces and the materials of the two bodies.

The first term in (1) represents elastic response of the interface, while the second damping term models dissipation of energy during normal oscillations. The nature of this dissipation is fairly complex, and the term in (1) is only presumed to model the overall damping effect produced by the viscous properties of surface asperities, contaminants, and lubricants. The coefficients b_N and l_N are usually assumed to be constant [see Hunt and Crossley, 1975; Oden and Martins, 1985]. Some

studies of variable damping coefficients were presented by *Tworzydło and Becker* [1991].

The second constitutive equation of the interface is a friction law of the form:

$$\begin{aligned} a < 0 &\Rightarrow \sigma_T = 0 \\ a \geq 0 &\Rightarrow |\sigma_T| \leq c_T(a)^{m_T} : \\ &|\sigma_T| < c_T(a)^{m_T} \Rightarrow \dot{d} = 0 \\ &|\sigma_T| = c_T(a)^{m_T} \Rightarrow \dot{d} = -\lambda\sigma_T \quad (\lambda \geq 0) \end{aligned} \quad (2)$$

where \dot{d} is the sliding velocity calculated as the time derivative of sliding distance and the index T indicates a direction tangential to the contact surface. The friction force is a function of the normal approach of the two surfaces, which in turn depends on the normal force. The actual value of the static coefficient of friction can be expressed by

$$\mu = \frac{c_T}{c_N} a^{(m_T - m_N)} \quad (3)$$

so that if $m_T = m_N$, this model represents Coulomb friction law with $\mu = c_T/c_N$. In terms of normal stress on the interface, equation (3) can be recast in the form

$$\mu = \frac{c_T}{\frac{c_N^{m_T}}{m_T}} (-\sigma_N)^{\frac{m_T}{m_N} - 1} \quad (4)$$

where it was assumed that $\dot{a} = 0$ (static friction).

An important observation is that within this model the value of friction force is not uniquely defined in terms of displacements or velocities (in particular at zero sliding velocity). In order to avoid numerical difficulties resulting from this fact, the friction law is usually regularized by approximating the friction model with a continuously differentiable function [*Oden and Martins*, 1985]. One possible form of regularized friction law for this kind of problem is

$$\sigma_T = c_T a^{m_T} \Phi_\epsilon(\dot{d}),$$

where

$$\Phi_\epsilon(\xi) = \begin{cases} \left(2 - \left|\frac{\xi}{\epsilon}\right|\right) \frac{\xi}{\epsilon} & \text{if } |\xi| \leq \epsilon \\ \text{sgn } \xi & \text{if } |\xi| > \epsilon \end{cases} \quad (5)$$

is the regularization function, ϵ is a regularization parameter, and sgn in the sign function.

4. Numerical Model for Studies of Stick-Slip Motion

In this section we present a numerical model used for studies of rock blocks with a compliant interface and

Oden-Martins friction model sliding on a flat surface. The motion of a large granite block supported by a set of springs (K_x , K_y , and K_θ) and sliding on a moving flat surface (Figure 1) is analyzed. The flat surface is assumed to be moving with a constant velocity \dot{U} . Symmetry with respect to the xy plane is assumed, and therefore motion is confined to this plane.

Figure 1

Block A is assumed to be rigid; hence 3 degrees of freedom (two translations and a rotation) are needed to describe its motion. It is important to emphasize that not only the tangential motion of the slider (the block) is analyzed, but its normal and rotational degrees of freedom are analyzed as well. The equations of motion of the block in this case are

$$\mathbf{M}\ddot{\mathbf{u}}(t) + \mathbf{C}\dot{\mathbf{u}}(t) + \mathbf{K}\mathbf{u}(t) + \mathbf{P}_N[\mathbf{u}(t), \dot{\mathbf{u}}(t)] + \mathbf{P}_T[\mathbf{u}(t), \dot{\mathbf{u}}(t)] = \mathbf{F}(t) \quad (6)$$

In (6),

- $\mathbf{u}, \dot{\mathbf{u}}, \ddot{\mathbf{u}}$ column vectors of discrete displacements, velocities, and accelerations of the center of mass of the block;
- $\mathbf{M}, \mathbf{C}, \mathbf{K}$ mass, damping, and stiffness matrices;
- \mathbf{F} load vector corresponding to body forces applied at the center of mass of the block (such as gravitational loads, etc.);
- $\mathbf{P}_N, \mathbf{P}_T$ vector of consistent (i.e., computed accurately by integrating tractions on the appropriate contact surfaces) forces due to normal and frictional response of the interface, respectively.

For the discrete rigid body model, these vectors and matrices are given by

$$\begin{aligned} \mathbf{u} &= \{u_x, u_y, u_\theta\}^T \\ \mathbf{F} &= \{F_x, F_y, F_\theta\}^T \\ \mathbf{M} &= \begin{bmatrix} M_x & 0 & 0 \\ 0 & M_y & 0 \\ 0 & 0 & J \end{bmatrix} \\ \mathbf{C} &= \begin{bmatrix} C_x & 0 & 0 \\ 0 & C_y & 0 \\ 0 & 0 & C_\theta \end{bmatrix} \\ \mathbf{K} &= \begin{bmatrix} K_x & 0 & 0 \\ 0 & K_y & 0 \\ 0 & 0 & K_\theta \end{bmatrix} \\ \mathbf{P}_N &= \{0, P_{Ny}, P_{N\theta}\}^T \end{aligned}$$

$$\mathbf{P}_T = \{P_{Tx}, 0, P_{T\theta}\}^T,$$

where

$$\begin{aligned} P_{Ny} &= B \int_{-\frac{L}{2}}^{\frac{L}{2}} [c_N u_s^{m_N} + b_N u_s^{l_N} \dot{u}_s] ds \\ P_{N\theta} &= B \int_{-\frac{L}{2}}^{\frac{L}{2}} [c_N u_s^{m_N} + b_N u_s^{l_N} \dot{u}_s] s ds \\ P_{Tx} &= B c_T \Phi_\epsilon (\dot{u}_x + \frac{H}{2} \dot{u}_\theta - \dot{U}) \int_{-\frac{L}{2}}^{\frac{L}{2}} u_s^{m_T} ds \\ P_{T\theta} &= \frac{H}{2} P_{Tx}, \end{aligned}$$

and

$$u_s = u_y - s u_\theta, \quad \dot{u}_s = \dot{u}_y - s \dot{u}_\theta$$

The block is of dimensions $L \times H \times B$, B being the out-of-plane dimension. The dampers C_x, C_y , and C_θ (not shown in Figure 1 for clarity) represent external damping effects of the surroundings on the motion of the block. From the above formulae, it is clear that integrating contact and friction tractions over the contact surface produces resultant frictional and normal forces as well as a torque acting on the block.

4.1. Methodology for Transient Nonlinear Analysis

A precise study of the fully nonlinear frictional behavior of the system will be performed via the transient solution of the equations of motion (6). These equations represent a highly nonlinear set of second order differential equations for the unknown displacements \mathbf{u} as a function of time. There exists a variety of numerical integration methods for such systems. Details of formulation, stability conditions, and applicability of these methods can be found in many references [see, e.g., *Oden and Martins*, 1985; *Oden et al.*, 1989].

In this work, the solution of the set of equations (6), subjected to the initial conditions $\mathbf{u}(0) = \mathbf{u}_0$ and $\dot{\mathbf{u}}(0) = \dot{\mathbf{u}}_0$, is performed using Newmark's method as presented by *Oden and Martins* [1985]. For extremely small overall sliding velocities \dot{U} encountered in earthquake simulations, while the movement of the block is very slow and smooth during the stick phase, it may become very fast and violent during the unstable slip phase. Therefore, to optimize the solution process of the nonlinear set of equations (6), additional numerical techniques were developed and implemented. These techniques, based on the current numerical solution and its estimated error as well as the status of the problem, will adapt some parameters of the numerical model for optimal convergence and improved accuracy. In the current work, the following procedures are used: Adaptive sizing of the time step and adaptive sizing of the regularization parameter ϵ .

When convergence is detected at a time step, an approximate temporal error indicator is computed and compared to a specified maximum. If the error is greater than the maximum, the step size is reduced by a specified factor, and the solution is repeated over the same step. If, on the other hand, the temporal error is less than the maximum, the solution process is advanced to the next step. In this case, however, the step size is modified in such a way that makes the value of the temporal error close to a specified optimal value. This simple procedure will effectively adjust the size of the time step from very small in the slip phase to large during the stick phase.

In addition, owing to the wide range of velocities encountered, another adaptive procedure was necessary. The very small values of velocities during the stick phase necessitate that the regularization parameter ϵ be assigned extremely small values. When the slider's velocity dramatically increases in the slip phase it becomes, with these values of ϵ , numerically difficult to capture and return into the regularized stick zone at the end of slip. Instead, a numerical phenomenon occurs in which the solution alternates between slip to the right and slip to the left and vice versa, never entering into the stick phase. This is purely a numerical phenomenon, where the solution at a single time step jumps "over" the regularized stick zone without "noticing" it. While this can be remedied with extremely small values of time steps, it is more efficient to adjust the regularization parameter to the current range of sliding velocities. Therefore another adaptive procedure was devised and used to adjust the value of the regularization parameter, ϵ , at each time step.

The two adaptive procedures, while not jeopardizing the accuracy of the results, improve convergence and reduce the number of necessary time steps. For more details, the reader is referred to *Tworzydło et al.* [1995].

Another simplified solution procedure is also used to estimate the stability of frictional sliding. Let the nonlinear equations of motion (6) be linearized around a prescribed configuration of the system, defined by

$$\{\ddot{\mathbf{u}}_R, \dot{\mathbf{u}}_R, \mathbf{u}_R\}^T = \{0, 0, \mathbf{u}_R\}^T, \text{ as}$$

$$\mathbf{M}\ddot{\mathbf{u}} + (\mathbf{C} + \mathbf{C}^N + \mathbf{C}^T)\dot{\mathbf{u}} + (\mathbf{K} + \mathbf{K}^N + \mathbf{K}^T)(\mathbf{u} - \mathbf{u}_R) = \Delta\mathbf{F}, \quad (7)$$

where

$$\mathbf{C}^N = \frac{\partial \mathbf{P}_N}{\partial \dot{\mathbf{u}}}, \quad \mathbf{C}^T = \frac{\partial \mathbf{P}_T}{\partial \dot{\mathbf{u}}}, \quad \mathbf{K}^N = \frac{\partial \mathbf{P}_N}{\partial \mathbf{u}}, \quad \mathbf{K}^T = \frac{\partial \mathbf{P}_T}{\partial \mathbf{u}} \quad (8)$$

Equations (7) are reduced and solved for the steady state sliding equilibrium position (i.e., $\ddot{\mathbf{u}} = \mathbf{0}$, and $\dot{\mathbf{u}} =$

0). At this position, an eigenanalysis is performed on the linearized equations by solving the eigenproblem:

$$[\mathbf{M}\lambda^2 + (\mathbf{C} + \mathbf{C}^N + \mathbf{C}^T)\lambda + (\mathbf{K} + \mathbf{K}^N + \mathbf{K}^T)]\Phi = \mathbf{0}, \quad (9)$$

where λ are the eigenvalues and Φ are the eigenvectors. Owing to the existence of friction and the nonsymmetry of the equations, the eigenvalues and vectors are usually complex. Investigation of the eigensolution of the system leads to estimation of both the stability of sliding and the frequencies of different modes of oscillations. This method of stability analysis, although approximate, is clearly more economic than the full transient analysis, in particular for realistic more complicated systems. The interested reader is referred to *Oden and Martins* [1985], *Tworzydło and Becker* [1991], and *Tworzydło et al.* [1994] for more details on the analysis method.

5. Numerical Studies

In this section we present numerical examples that illustrate the ideas discussed earlier. In particular, we analyze granite blocks sliding on moving granite flat surfaces. We model both stable and unstable behaviors. In the process, both micro and macroscale phenomena are investigated. In addition, we show the results of a parametric study of critical stiffnesses and damping coefficients that separate stable and unstable behaviors.

A sample of Westerly granite with in-plane dimensions of $L \times H = 0.8 \times 0.2$ m, and out-of-plane dimension of $B = 0.15$ m, is considered. This block is representative of rocks used in some previous experimental studies. Using a typical value for the mass density of granite, the following dynamic properties of the block are defined:

$$M_x = M_y = 62.4 \text{ kg}, \quad J = 3.536 \text{ kg m}^2$$

The following interface parameters, representative of the friction of two Westerly granite surfaces, are used:

$$\begin{aligned} c_N &= 5.0 \times 10^4 \text{ kg s}^{-2} \text{ m}^{3.5}, \\ b_N &= 0, \\ m_N &= m_T = l_N = 2.5 \end{aligned}$$

The above constants were obtained by a simplified version of statistical methods [*Oden and Tworzydło*, 1997; *Tworzydło et al.*, 1993] that utilize statistical properties of real surface profiles on a ground piece of rock [Power et al., 1988]. The coefficient of friction is assumed to be $\mu = 0.7$, so that

$$c_T = 3.5 \times 10^4 \text{ kg s}^{-2} \text{ m}^{3.5}$$

In the initial studies, the values of external stiffnesses and viscosities were assumed as follows:

$$\begin{aligned} K_x &= 23880.0 \text{ kg s}^{-2}, \quad K_y = 0, \quad K_\theta = 0, \\ C_x &= 300.0 \text{ kg s}^{-1}, \quad C_y = 150.0 \times 10^3 \text{ kg s}^{-1}, \\ C_\theta &= 250.0 \times 10^3 \text{ kg s}^{-1} \text{ m}. \end{aligned}$$

In actual experimental settings, the damping coefficients can be found by measuring the damping ratios in the different modes of free vibration tests. No specific experimental results were available here; therefore representative values were chosen so that the damping forces produced with these coefficients were within 10% of the forces applied on the block from other sources (spring and gravity loads), a ratio that we believe to be reasonable. The body forces consisted of gravitational loads only; i.e., $\mathbf{F} = \{F_x, F_y, F_\theta\}^T = \{0, 612.0, 0\}^T \text{ kg m s}^{-2}$. The velocity of the moving surface is quite slow:

$$\dot{U} = 1.0 \text{ } \mu\text{m s}^{-1}$$

The transient analysis of the motion of the block was performed starting from the equilibrium position ($\mathbf{u}_0 = \mathbf{0}$, $\dot{\mathbf{u}}_0 = \{\dot{U} \ 0 \ 0\}^T$). First, the block sticks to the moving surface and translates along with it. When the spring force exceeds the frictional capacity of the interface, either of two cases (stable or unstable sliding) may prevail depending on the properties of the block, the interface, and the system as a whole. In the first case, corresponding to the data described above, the block stays in its place sliding on the moving surface in what is called a stable mode. Figure 2 shows the motion of the center of mass of the block in the x direction. In this case, the coefficient of friction remains constant at its static value; that is, there is no reduction of the kinetic coefficient of friction (with the present friction model). The two blocks slide on each other at a constant, very slow velocity.

Figure 2

The behavior of the slider (the block), however, is very different in some other cases. If, for instance, the external damping coefficients are reduced to

$$\begin{aligned} C_x &= 30.0 \text{ kg s}^{-1}, \quad C_y = 1.5 \times 10^3 \text{ kg s}^{-1}, \\ C_\theta &= 25.0 \text{ kg s}^{-1} \text{ m}, \end{aligned}$$

the slider engages in what is called unstable stick-slip episodes. The slider in this case slips back under the influence of the spring force, releasing much of the stored

elastic energy of the system. Figure 3 shows the motion of the center of mass of the block in the tangential and normal directions for this case. At the end of the sliding phase, the slider sticks again to the moving surface and moves along with it. The process repeats itself again and again whenever the tangential force at the interface exceeds its frictional capacity. Synchronized with this stick-slip behavior in the tangential direction, the slider performs jumps normal to the surface, thus momentarily separating the two bodies and reducing the apparent coefficient of friction (see Figure 3). It should be noted that Figure 3 only represents an overall, macroscale behavior of the system. Detailed analysis of the motion in the slip phase is discussed below. On a real fault system, the slip event and the associated energy release correspond to an earthquake, and the stick phase is the quiet period between earthquakes (when energy buildup takes place).

Figure 3

In the present model, this phenomenological unstable sliding of the block is a consequence of an interesting microscale high-frequency behavior illustrated in Figure 4. In an unstable sliding system, when the frictional force attains its maximum (at the end of stick phase) the slider engages in vibrations at high frequencies and low amplitudes. These vibrations are unstable and are caused by frictional coupling of normal and rotational modes of the slider.

Figure 4

The coupled growth of microoscillations is illustrated in Figure 4 which clearly shows synchronized normal and rotational oscillations. These unstable oscillations grow quickly, and the slider actually begins to perform very short duration sticks and slips. Figure 4 shows enlarged segments of the history of the displacements of the block in the tangential, normal, and rotational directions at the inception of the slip stage. It also shows the growth of the relative sliding velocity ($\dot{u}_x - \dot{U}$) at the interface. A zero relative sliding velocity indicates a stick condition. In Figure 5 one of the cycles of Figure 4 is shown with higher timescale resolution. To illustrate the nature of motion of the block, Figure 6 shows a sequence of drawings of the block with exaggerated displacements and rotations at nine time steps within the cycle of Figure 5.

Figure 5

Figure 6

It is important to notice that the microsticks and microslips have very high frequencies and infinitesimal amplitudes, so that they cannot be observed by the naked eye, and the motion of the slider is perceived as swift macroscopic sliding toward the spring, as shown in Figure 3. The entire slip event has lasted for about 10 s.

In large deformable systems, it is expected that the

normal oscillations or even separations between the two surfaces may take place locally and can travel as a high-speed wave along the interface. A somewhat similar phenomenon was observed in experiments on rubber friction and was referred to as waves of detachment [Schallamach, 1971].

To bring our simulations even closer to typical velocities of tectonic plates, we decrease the sliding velocity to become: $\dot{U} = 1.0 \times 10^{-3} \mu\text{m s}^{-1}$, which corresponds to approximately 31.5 mm yr^{-1} . The macroscopic behavior of the slider in this case resembles that of the previous one (depicted in Figure 3) except that the time scale is multiplied by 10^3 . Hence the slip events occur at intervals of about 147 days, and they also last for about 10 s. At the end of the slip event, the two bodies in contact have slipped relative to each other by a distance of 12.5 mm, approximately.

This predicted macroscopic behavior of stick-slip is in qualitative agreement with a broad collection of experimental observations reported by many researchers [Byerlee, 1967; Byerlee and Summers, 1975; King, 1994; Rice, 1982; Scholz et al., 1972; Tullis and Weeks, 1986]. Several rate and state constitutive models have been suggested and used to predict similar stick-slip phenomenon and the friction reduction associated with it [Rice and Tse, 1986; Ruina, 1983]. These models, however, produce not only the stick-slip kind of behavior but also other experimentally observed phenomena such as velocity dependence, hold time dependence of static friction, etc.

It is worthwhile noting that even in the potentially stable case, if a block sliding in a steady mode is intentionally perturbed strongly enough, it might lose contact with the moving surface and enter a different slip mode. In this case, the block performs few microscale jumps, sticks, and slips. This translates globally to macroslips which are different in nature than the self-excited case. The oscillations are damped out and the block stabilizes again unless another perturbation is applied. Figure 7 shows the nature of the normal oscillation that the block performs while it slips, which are clearly different from the jumps shown in Figure 4. The introduced intentional perturbation may be caused in practical cases by interlocking of sizeable asperities on the moving surfaces or by the arrival of a dynamic wave propagating through the block. This observation may suggest that a section of a fault that is in a stable sliding motion may become unstable if hit by an impulse from a nearby slip event.

It is of interest to study the influence of the overall stiffness and damping magnitude in the system on the

Figure 7

stability of sliding. The results of a brief study of this kind, illustrating the influence of selected parameters (one at a time) are presented below.

The distance that a block slides back is dependent, among other factors, on the spring stiffness K_x . For larger K_x , the block slips less. For very large K_x , however, the slip distance becomes very small, and the block seems to be sliding in a stable mode. Figure 8 shows on a log-log scale the slip distance the block travels every time it slips versus the normalized stiffness K_x/K_{x0} , where K_{x0} corresponds to the basic data introduced at the beginning of this section. It is evident from Figure 8 that for values of K_x beyond a certain level, the motion of the block is of a stable nature. This conclusion agrees well with the notion of critical stiffness discussed in previous works dedicated to stick-slip motion in rocks [Rice, 1982; Ruina, 1983; Tullis and Weeks, 1986].

Figure 8

Similarly, if the system is heavily damped in the normal direction (large C_y), the vertical oscillations of the slider are essentially eliminated, and the motion becomes stable. Figure 9 shows the amplitude of the slip distance versus the value of the external damping coefficient, normalized with respect to the value $C_{y0} = 1.5 \times 10^3 \text{ kg s}^{-1}$. It is clear that similar to the critical stiffness discussed above, there exists a critical damping beyond which the sliding becomes stable. Indeed, Scholz *et al.* [1972] showed experimentally that on clean ground rock surfaces (i.e., without the damping effect of the gouge), the stick-slip phenomenon becomes more pronounced. No attempt is made here to determine any relationship for the amount of normal damping necessary to suppress instability.

Figure 9

We now use the method of eigenanalysis of the linearized system to investigate the stability of sliding. To simplify the solution of the complex eigenproblem (equation (9)), the case with no damping is considered. This is a fair representation of the case of low damping.

The effect of the rotational stiffness (K_θ) on the stability of sliding is investigated by eigenanalysis of the linearized system. Figure 10 shows the frequencies of the different modes of vibration of the slider as a function of K_θ in the absence (Figure 10a) and presence (Figure 10b) of friction. It is clear that the presence of friction leads to coalescence of the normal and rotational frequencies (ω_y, ω_θ) at lower values of K_θ . The real parts of the complex eigenvalues (Figure 10c) are positive for lower K_θ . A positive real part indicates that the oscillations are expected to grow, thus promoting unstable behavior. The rate of growth of oscillations is exponentially proportional to the real part.

Figure 10

In other words, the presence of friction results in cou-

pling of the different degrees of freedom of the slider (namely normal and rotational) and in promoting instability. A close investigation of the history of the microoscillations, computed earlier by the full transient analysis (Figure 4), reveals that they occur at a frequency of about 660 Hz. The eigenanalysis of the undamped problem (Figure 10) predicts a frequency of about 770 Hz at $K_\theta = 0$.

For higher values of K_θ , on the other hand, the frequencies are not coupled, and the real parts vanish; this predicts stable sliding. It is worth mentioning that in the case of a highly restrained block (high stiffnesses), it is expected that the block's own deformations become more important and the assumption of a rigid block becomes less accurate.

The above studies are representative of systems with low damping levels. Application of heavier damping tends to suppress the vibrations of the system and at sufficient damping levels the sliding becomes stable, as shown in our numerical examples. We have not performed systematic studies of the level of the normal and rotational damping needed to completely suppress the unstable behavior of the system.

6. Conclusions

The stick-slip frictional behavior is modeled by a methodology that combines the Oden-Martins friction law with the full dynamic analysis of the system. The friction law recognizes the normal approach on a contact surface as an independent variable. This analysis, which incorporates not only the tangential degree of freedom but also the normal and the rotational ones, reveals much information about the macroscopic behavior of the system. The observed macroscopic behavior, slip events in particular, is a manifestation of the microscale behavior of the system.

The primary objective of this study was to clearly show that frictional sliding may become unstable even without explicit velocity or slip weakening in the friction law and that it could happen for typical rock blocks sliding at extremely low overall velocities in the range characteristic of the San Andreas fault. These unstable frictional phenomena were triggered by dynamic coupling of vibration modes of the system. A critical component in modeling of these unstable modes was a constitutive law recognizing the normal approach on the contact surface.

The inclusion of the normal and rotational degrees of freedom and corresponding oscillations may help explain some physical phenomena associated with the occurrence of earthquakes, such as the heat paradox, fluc-

tuations in groundwater levels, escape of hydrogen from the Earth's deep crust, and high mobility of very large landslides studied by *Melosh* [1979].

In the context of earthquakes we believe that the above methodology, when combined with more realistic models of rock friction, will contribute to extend the understanding of earthquake mechanisms and the methods of their dynamic modeling. It can be expected that the complexity of real situations will be much greater; additional challenges in the case of rock formations result from a different scale of problem, elastic wave propagation, complex geometries and material property distributions, and more complex and variable constitutive characteristics of interfaces (fault surfaces) of the kind actually observed in experimental studies of rocks [e.g., *Dieterich*, 1978, 1979a; *Ruina*, 1983; *Tullis and Weeks*, 1986]. On a real fault system, the pressures are very high, but so are all other parameters: stiffnesses, forces, masses, wave amplitudes, etc. Without an attempt to model them, it is difficult to predict what role the normal vibrations will have on real faults; however, we can speculate that they will be of importance.

Acknowledgments. The authors would like to acknowledge J.T. Oden, Texas Institute for Computational and Applied Mathematics, for his support and expertise on the subject of computational dynamic friction. This research was supported by the U.S. Geological Survey (USGS), Department of the Interior, under USGS award 1434-94-G-2414.

We also want to extend special thanks to the reviewers of the paper, in particular Terry E. Tullis, for their careful reviews and helpful comments.

References

- Andrews, D. J., Rupture propagation with finite stress in antiplane strain, *J. Geophys. Res.*, *81*, 3575–3582, 1976a.
- Andrews, D. J., Rupture velocity of plane strain shear cracks, *J. Geophys. Res.*, *81*, 5679–5687, 1976b.
- Aronov, V., A. F. D'Souza, S. Kallpakijan, and I. Shareef., Experimental investigation on the effect of system rigidity on wear and friction-induced vibrations, *J. of Lubric. Technol.*, *105*, 206–211, 1983.
- Aronov, V., A. F. D'Souza, S. Kallpakijan, and I. Shareef., Interaction among friction, wear and system stiffness, 1, Effect of normal load and system stiffness, 2, Vibrations induced by dry friction, 3, Wear model, *J. of Lubric. Technol.*, *106*, 54–69, 1984.
- Biegel, R. L., C. G. Sammis, and J. H. Dieterich., The frictional properties of a simulated gouge having a fractal particle distribution, *J. of Struct. Geol.*, *11*(7), 827–846, 1989.
- Blanpied, M.L., D.A. Lockner, and J.D. Byerlee., Fault stability inferred from granite sliding experiments at hydrothermal conditions, *Geophys. Res. Lett.*, *18*, 609–612, 1991.
- Brune, J., S. Brown, and P. Johnson., Rupture mechanism

- and interface separation in foam rubber models of earthquakes: A possible solution to the heat flow paradox and the paradox of large overthrusts, *Tectonophysics*, 218, 59–67, 1993.
- Byerlee, J. D., Frictional characteristics of granite under high confining pressure, *J. Geophys. Res.*, 72, 3639–3648, 1967.
- Byerlee, J. D., and R. Summers., Stable sliding preceding stick-slip on fault surfaces at high pressure, *Pure Appl. Geophys.*, 113, 63–68, 1975.
- Cao, T., and K. Aki., Seismicity simulation with a rate- and state-dependent friction law, *Pure Appl. Geophys.*, 124, 487–513, 1986.
- Carlson, J. M., J. S. Langer, B. E. Shaw, and C. Tang., Intrinsic properties of a burridge-knopoff model of an earthquake fault, *Phys. Rev. A, Gen. Phys.*, 44(2), 884–897, 1991.
- Day, S., Three-dimensional finite difference simulation of fault dynamics: Rectangular faults with fixed rupture velocity, *Bull. Seismol. Soc. Am.*, 72, 705–727, 1982a.
- Day, S., Three-dimensional simulation of spontaneous rupture: The effect of nonuniform prestress, *Bull. Seismol. Soc. Am.*, 72, 1881–1902, 1982b.
- Dieterich, J. H., Time-dependent friction and the mechanics of stick slip, *Pure Appl. Geophys.*, 116, 790–806, 1978.
- Dieterich, J. H., Modeling of rock friction, 1, Experimental results and constitutive equations, *J. Geophys. Res.*, 84, 2161–2168, 1979a.
- Dieterich, J. H., Modeling of rock friction, 2, Simulation of preseismic slip, *J. Geophys. Res.*, 84, 2169–2175, 1979b.
- D’Souza, A., and A. Dweib., Self-excited vibrations induced by dry friction, 2, Stability and limit cycle analysis, *J. Sound Vibration*, 137(2), 177–190, 1990.
- Dweib, A., and A. D’Souza., Self-excited vibrations induced by dry friction, 1, Experimental study, *J. Sound Vibration*, 137(2), 163–175, 1990.
- Hunt, K. H., and F. R. E. Crossley., Coefficient of restitution interpreted as damping in vibroimpact, *J. of Appl. Mech.*, 42, 440–445, 1975.
- King, C.-Y., Earthquake mechanism and predictability shown by a laboratory fault, *Pure Appl. Geophys.*, 143, 457–482, 1994.
- Lockner, D. A., R. Summers, and J. D. Byerlee., Effects of temperature and sliding rate on frictional strength of granite, *Pure Appl. Geophys.*, 124, 445–469, 1986.
- Melosh, H. J., Acoustic fluidization: A new geologic process, *J. Geophys. Res.*, 84, 7513–7520, 1979.
- Oden, J. T., and J. A. C. Martins., Models and computational methods for dynamic friction phenomena, *Comput. Methods Appl. Mech. Eng.*, 52, 527–634, 1985.
- Oden, J. T., and W. Tworzydło., Computational micro- and macroscopic models of contact and friction, 1, Formulation and approach, *Wear*, in press, 1997.
- Oden, J. T., J. Martins, W. Tworzydło, S. Wu, and L. White., Progress in theory and modeling of friction and in the control of dynamic systems with friction forces, technical report, Air Force Off. of Sci. Res., Bolling AFB, D.C., 1989.
- Power, W. L., T. E. Tullis, and J. D. Weeks., Roughness and wear during brittle faulting, *J. Geophys. Res.*, 93, 15,268–15,278, 1988.
- Rice, J. R., Shear instability in relation to the constitutive

- description of fault slip, lecture presented at Seismicity in Mines Symposium, International Society for Rock Mechanics and South African Institute of Mining and Metallurgy, Johannesburg, South Africa, Nov. 1982.
- Rice, J. R., Spatio-temporal complexity of slip on a fault, *J. Geophys. Res.*, *98*, 9885–9907, 1993.
- Rice, J. R., and J. Gu., Earthquake aftereffects and triggered seismic phenomena, *Pure Appl. Geophys.*, *121*, 187–219, 1983.
- Rice, J. R., and A. Ruina., Stability of steady frictional slipping, *J. of Appl. Mech.*, *50*, 343–349, 1983.
- Rice, J. R., and S. T. Tse, Dynamic motion of a single degree of freedom system following a rate and state dependent friction law, *J. Geophys. Res.*, *91*, 521–530, 1986.
- Ruina, A., Slip instability and state variable friction laws, *J. Geophys. Res.*, *88*, 10,359–10,370, 1983.
- Ruina, A. L., Constitutive relations for frictional slip, edited by Z. Bazant, *Mechanics of Geomaterials*, pp. 163–187, John Wiley and Sons, 1985.
- Schallamach, A., How does rubber slide?, *Wear*, *17*, 301–312, 1971.
- Scholz, C., P. Molnar, and T. Johnson., Detailed studies of frictional sliding of granite and implications for the earthquake mechanism, *J. Geophys. Res.*, *77*, 6392–6406, 1972.
- Soom, A., and C. Kim., Interactions between dynamic normal and frictional forces during unlubricated sliding, *J. of Lubric. Technol.*, *105*, 221–229, 1983.
- Stesky R., Mechanisms of high-temperature frictional sliding in westerly granite, *Can. J. of Earth Sci.*, *15*, 361–375, 1978.
- Stuart, W. D., and G. M. Mavko., Earthquake instability on a strike-slip fault, *J. Geophys. Res.*, *84*, 2153–2160, May 1979.
- Tolstoi, D. M., Significance of the normal degree of freedom and natural normal vibrations in contact friction, *Wear*, *10*, 199–213, 1967.
- Tolstoi, D. M., G. A. Borisova, , and S. R. Grigorova., Role of intrinsic contact oscillations in normal direction during friction, in *Nature of the Friction of Solids*, p. 116, Nauka i Technika, Minsk, Russia, 1971.
- Tullis, T. E., and J. D. Weeks., Constitutive behavior and stability of frictional sliding of granite, *Pure Appl. Geophys.*, *124*, 383–414, 1986.
- Tworzydło, W. W., and E. B. Becker., Influence of forced vibrations on the static coefficient of friction – numerical modeling, *Wear*, *143*, 175–196, 1991.
- Tworzydło, W. W., E. B. Becker, and J. T. Oden., Numerical modeling of friction-induced vibrations and dynamic instabilities, edited by R. A. Ibrahim and A. Soom, *Friction-Induced Vibration, Chatter, Squeal and Chaos*, pp. 13–32, Am. Soc. Mech. Eng., New York, 1992.
- Tworzydło, W. W., J. T. Oden, W. Cecot, and C. Yew., New micro- and macroscopic models of contact and friction, in *Contact Problems and Surface Interaction in Manufacturing and Tribological Systems*, *PED – Publ. Am. Soc. Mech. Eng.*, *67*, 87–104, 1993.
- Tworzydło, W. W., E. B. Becker, and J. T. Oden., Numerical modeling of friction-induced vibrations and dynamic instabilities, *Appl. Mech. Rev.*, *47*(7), 255–274, 1994.
- Tworzydło, W. W., O. N. Hamzeh, and J. T. Oden., Modeling and prediction of earthquakes as unstable phenomena of dynamic friction, technical report, Comput. Mech.

Comp., Inc., Austin, Tex., 1995.

O. N. Hamzeh and W. W. Tworzydło, Computational Mechanics Company, Inc., 7800 Shoal Creek, Suite 290 E, Austin, Texas 78757. (e-mail: osama@comco.com; woytek@comco.com)

(Received May 13, 1996; revised April 10, 1997; accepted April 17, 1997.)

Copyright 1997 by the American Geophysical Union.

Paper number 97JB01167.
0148-0227/97/97JB-01167\$09.00

Figure 1. A block sliding with friction on a moving flat surface (flat fault).

Figure 1. A block sliding with friction on a moving flat surface (flat fault).

Figure 2. Stable sliding of a granite block on a moving surface.

Figure 2. Stable sliding of a granite block on a moving surface.

Figure 3. Macroscale stick-slip motion of an unstable granite block (at its center of mass) sliding on a moving surface ($\dot{U} = 1.0 \mu\text{m s}^{-1}$): (a) tangential displacement history and (b) normal displacement history.

Figure 3. Macroscale stick-slip motion of an unstable granite block (at its center of mass) sliding on a moving surface ($\dot{U} = 1.0 \mu\text{m s}^{-1}$): (a) tangential displacement history and (b) normal displacement history.

Figure 4. (a) Growth of tangential microscale sticks and slips, (b) normal jumps, (c) in-plane rotations, and (d) the relative tangential velocity at the interface of the granite block at the inception of the macroscopic slip phase.

Figure 4. (a) Growth of tangential microscale sticks and slips, (b) normal jumps, (c) in-plane rotations, and (d) the relative tangential velocity at the interface of the granite block at the inception of the macroscopic slip phase.

Figure 5. History of (a) tangential and (b) normal displacements, and (c) in-plane rotations of the granite block during one micro cycle of the slip event.

Figure 5. History of (a) tangential and (b) normal displacements, and (c) in-plane rotations of the granite block during one micro cycle of the slip event.

Figure 6. A plot showing the position of the block (with exaggerated displacements and rotations) at sequential time steps within the microcycle of Figure 5.

Figure 6. A plot showing the position of the block (with exaggerated displacements and rotations) at sequential time steps within the microcycle of Figure 5.

Figure 7. Microscale normal jump and oscillations of a stable granite block on moving surface due to external perturbation ($u_y < 0$ corresponds to separation).

Figure 7. Microscale normal jump and oscillations of a stable granite block on moving surface due to external perturbation ($u_y < 0$ corresponds to separation).

Figure 8. The slip distance of the granite block vs. the spring stiffness in the x direction. $K_{x0} = 23,880.0 \text{ kg s}^{-2}$.

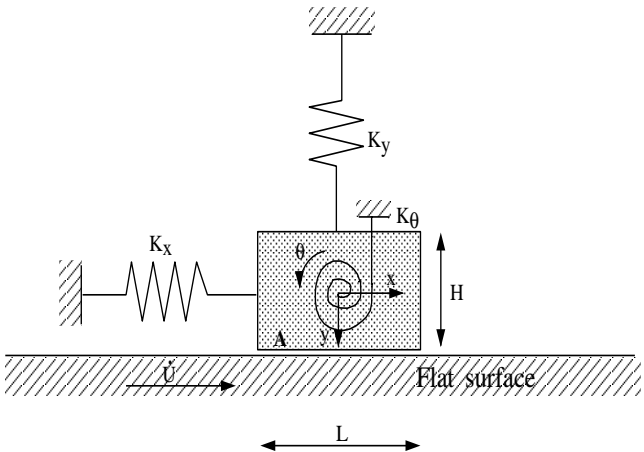
Figure 8. The slip distance of the granite block vs. the spring stiffness in the x direction. $K_{x0} = 23,880.0 \text{ kg s}^{-2}$.

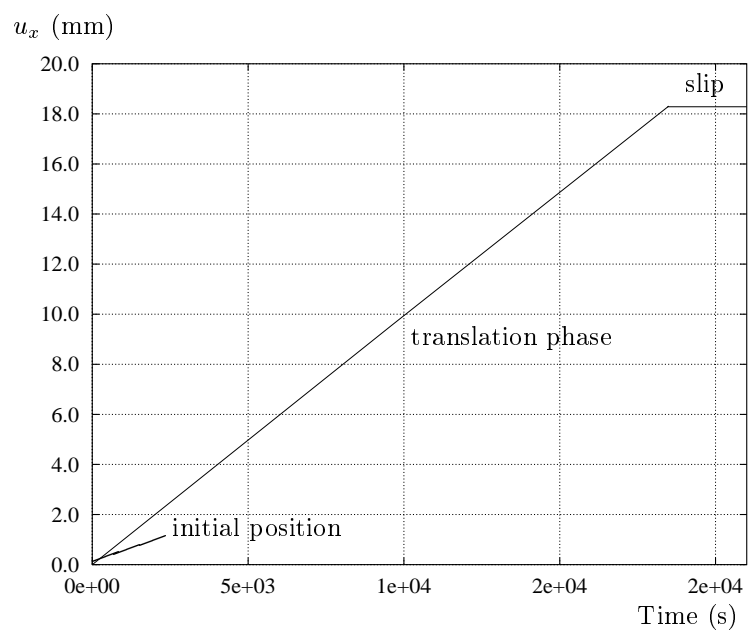
Figure 9. The slip distance of the granite block vs. the damping coefficient in the y direction. $C_{y0} = 1.5 \times 10^3 \text{ kg s}^{-1}$.

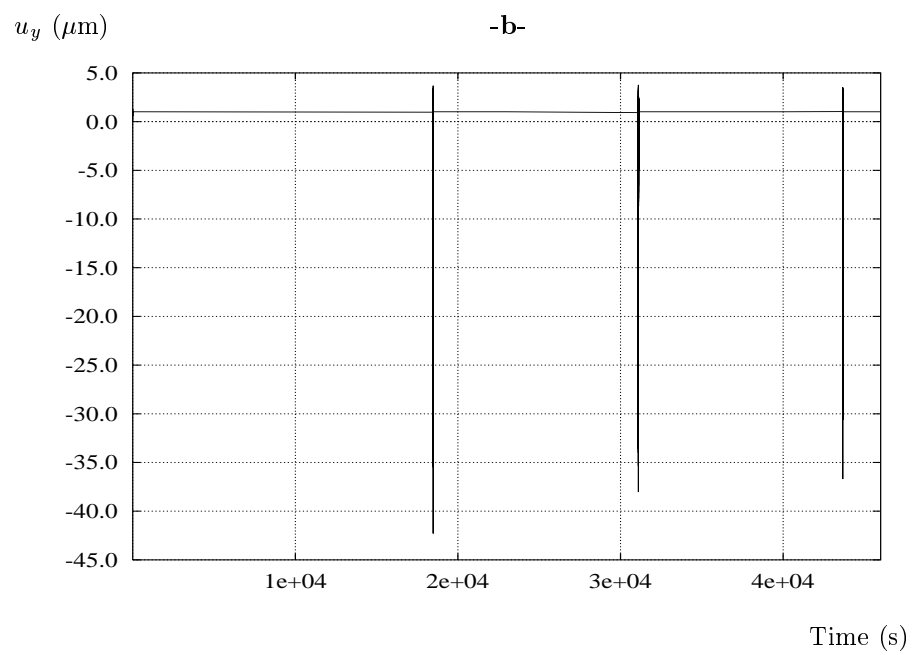
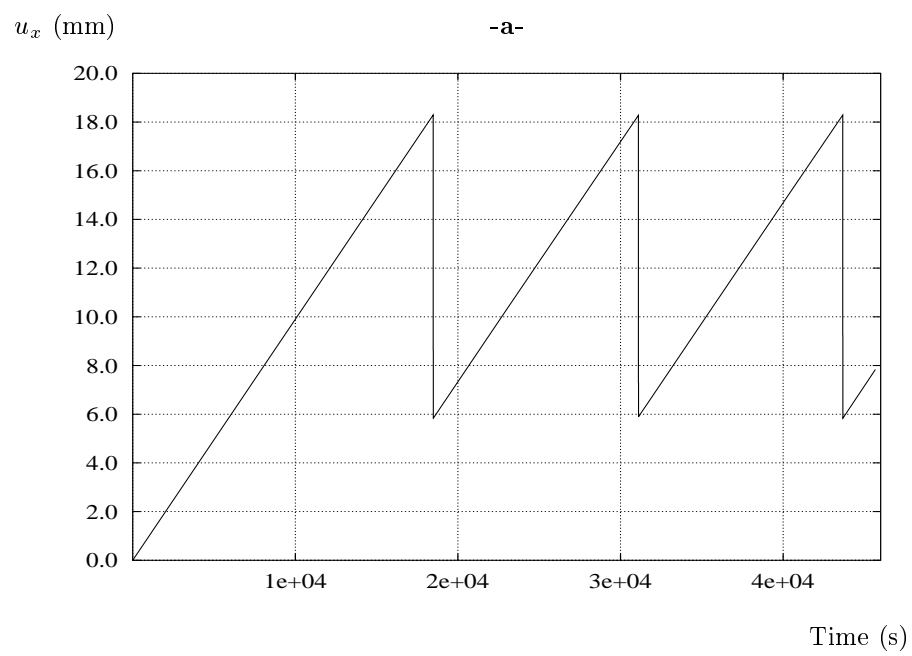
Figure 9. The slip distance of the granite block vs. the damping coefficient in the y direction. $C_{y0} = 1.5 \times 10^3 \text{ kg s}^{-1}$.

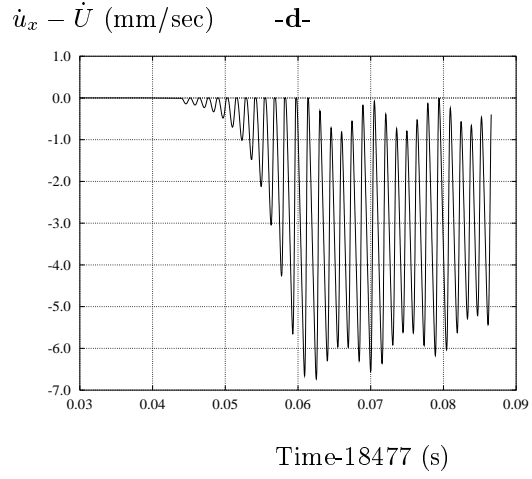
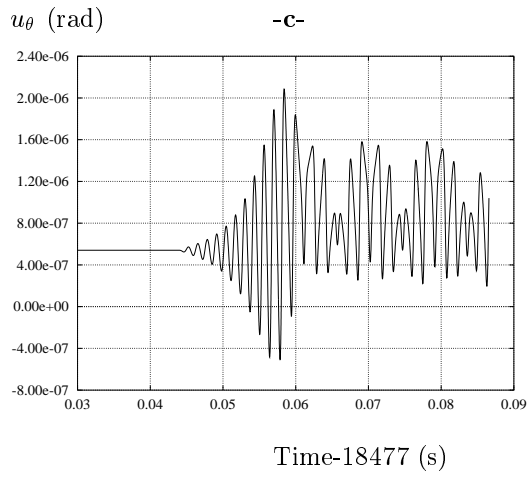
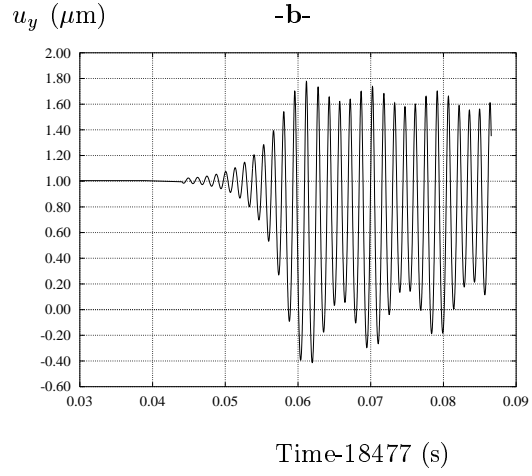
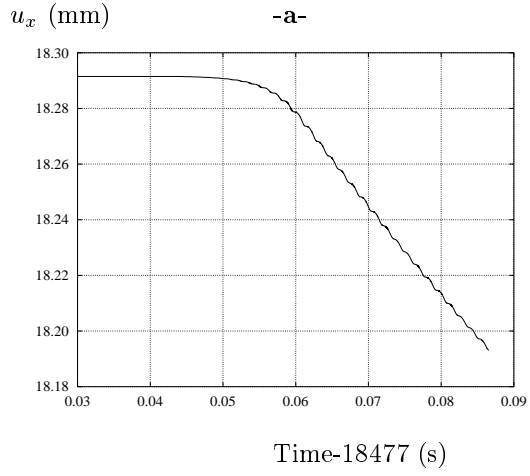
Figure 10. The results of the eigenanalysis of the block as the rotational stiffness is increased: (a) frequencies in the absence of friction, (b) frequencies with friction, and (c) real parts with friction.

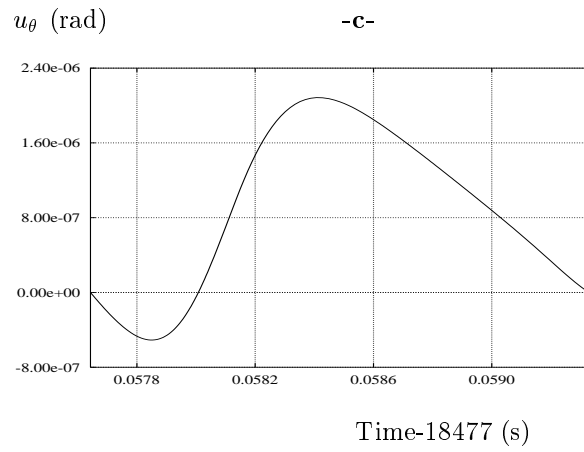
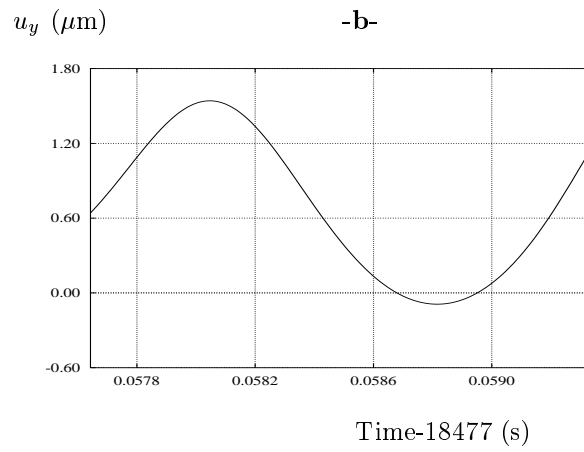
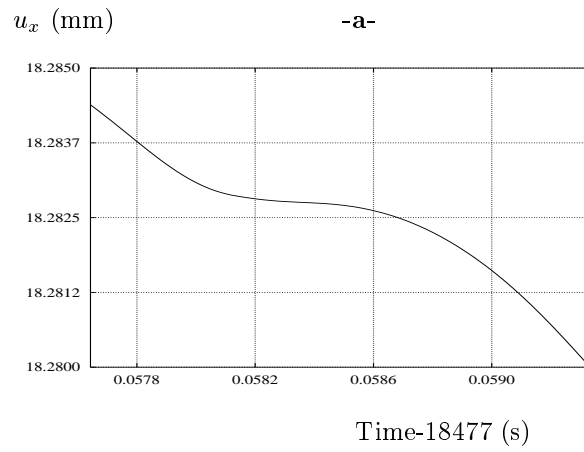
Figure 10. The results of the eigenanalysis of the block as the rotational stiffness is increased: (a) frequencies in the absence of friction, (b) frequencies with friction, and (c) real parts with friction.

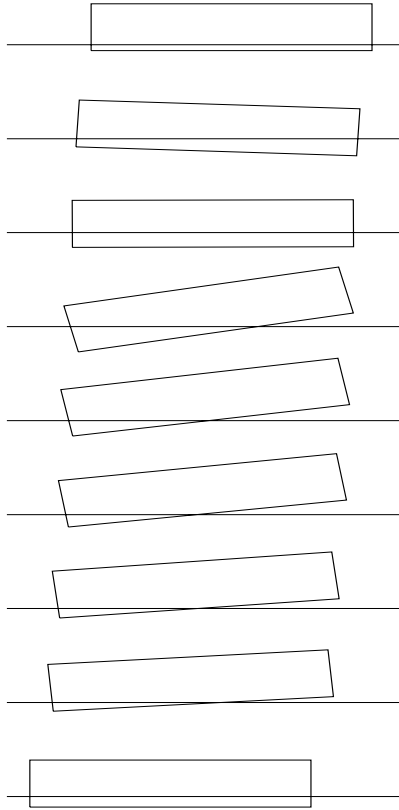


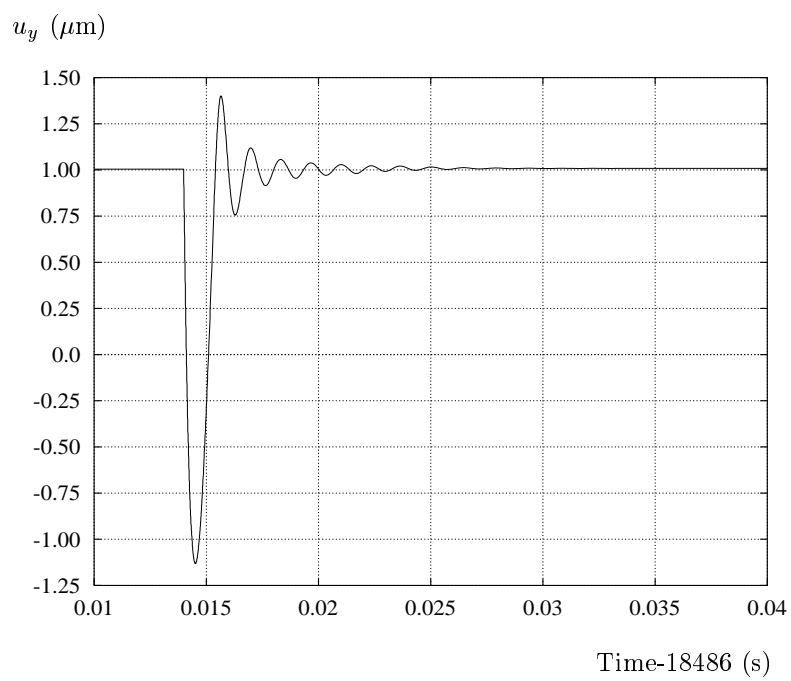




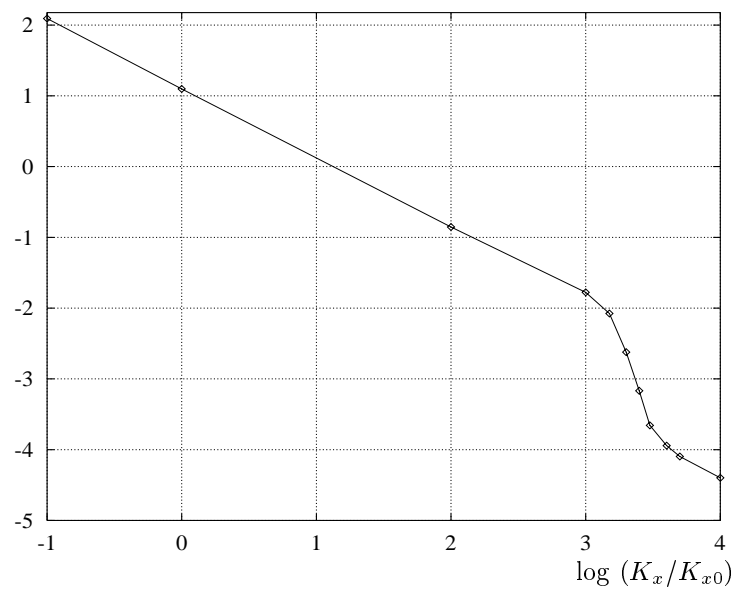








log (Slip distance in mm)



Slip distance in mm (log)

